ARCHIVIO ISTITUZIONALE DELLA RICERCA

Alma Mater Studiorum Università di Bologna
Archivio istituzionale della ricerca

Modulation of the Excited States of Ruthenium(II)-perylene Dyad to Access Near-IR Luminescence, Long-Lived Perylene Triplet State and Singlet Oxygen Photosensitization

This is the final peer-reviewed author's accepted manuscript (postprint) of the following publication:

Published Version:
Campos, I.S., Fermi, A., Ventura, B., Moraes, C.A.F., Ribeiro, G.H., Venâncio, T., et al. (2024). Modulation of the Excited States of Ruthenium(II)-perylene Dyad to Access Near-IR Luminescence, Long-Lived Perylene Triplet State and Singlet Oxygen Photosensitization. INORGANIC CHEMISTRY, 63(10), 4595-4603 [10.1021/acs.inorgchem.3c04145].

Availability:
This version is available at: https://hdl.handle.net/11585/966320 since: 2024-03-15

Published:

DOI: http://doi.org/10.1021/acs.inorgchem.3c04145

Terms of use:

Some rights reserved. The terms and conditions for the reuse of this version of the manuscript are specified in the publishing policy. For all terms of use and more information see the publisher's website.

This item was downloaded from IRIS Università di Bologna (https://cris.unibo.it/).
When citing, please refer to the published version.

(Article begins on next page)

16 September 2026

This is the final peer-reviewed accepted manuscript of:

Modulation of the Excited States of Ruthenium(II)-perylene Dyad to Access Near-IR Luminescence, Long-Lived Perylene Triplet State and Singlet Oxygen Photosensitization

I. A. S. Campos, A. Fermi, B. Ventura, C. A. F. Moraes, G. H. Ribeiro, T. Venâncio, P. Ceroni, R. M. Carlos *Inorg. Chem.* **2024**, *63*, 10, 4595–4603

The final published version is available online at:

https://doi.org/10.1021/acs.inorgchem.3c04145

Terms of use:

Some rights reserved. The terms and conditions for the reuse of this version of the manuscript are specified in the publishing policy. For all terms of use and more information see the publisher's website.

This item was downloaded from IRIS Università di Bologna (https://cris.unibo.it/)

When citing, please refer to the published version.

Modulation of the Excited States of Ruthenium(II)-perylene Dyad to Access Near-IR Luminescence, Long-Lived Perylene Triplet State and Singlet Oxygen Photosensitization

Isabele S. Campos, Andrea Fermi, Barbara Ventura, Carlos A. F. Moraes, Gabriel H. Ribeiro, Tiago Venâncio, Paola Ceroni,* and Rose M. Carlos*

Herein, we present a novel ruthenium(II)-perylene dyad (RuPDI-Py) that combines the photophysical properties of pyrrolidine-substituted perylene diimide (PDI-Py) and the ruthenium(II) polypyridine complex [Ru(phen)3]2+ . A comprehensive study of excited-state dynamics was carried out using time-resolved and steady-state methods in a dimethyl sulfoxide solution. The RuPDI-Py dyad demonstrated excitation wavelength-dependent photophysical behavior. Upon photoexcitation above 600 nm, the dyad exclusively exhibits the near-infrared (NIR) fluorescence of the 1PDI-Py state at 785 nm (τfl = 1.50 ns). In contrast, upon photoexcitation between 350 and 450 nm, the dyad also exhibits a photoinduced electron transfer from the {[Ru(phen)3]2+} moiety to PDI-Py, generating the charge-separated intermediate state {Ru(III)-(PDI-Py)•−} (4 μs). This state subsequently decays to the long-lived triplet excited state 3PDI-Py (36 μs), which is able to sensitize singlet oxygen (1O2). Overall, tuning 1O2 photoactivation or NIR fluorescence makes RuPDI-Py a promising candidate for using absorbed light energy to perform the desired functions in theranostic applications.

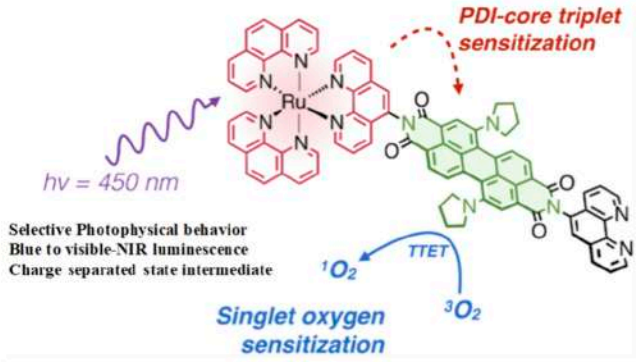

INTRODUCTION

Over the past decades, various studies have highlighted the ability of electron donor−acceptor systems (D−A) based on perylene diimide (PDI) chromophores to participate in photoinduced energy and electron transfer processes.[1−5] A fundamental issue that should be considered in planning a rational molecular array based on PDI is developing a D−A system capable of light harvesting in the visible to near-infrared (NIR) region and a strategy to access the long-lived triplet state of PDI.[6] These features are essential for the performance of PDI and open the opportunity to develop new D−A systems with advanced and specific properties. The relevance of these studies has intensified interest in playing on substituents at both the bay and imide positions of PDI, which, in addition to providing solubility and spatial arrangement, enable access to specific properties and functions.

For instance, singlet oxygen ($^1O_2$) production in toluene has been reported for a series of PDI derivatives with donor groups attached to aromatic bay positions and long alkyl groups at the *N*-imide position. The efficiency of $^1O_2$ formation is dependent on the substituent attached to PDI and is attributed to a decrease of the lowest singlet and triplet energy gap and to an increase of the spin−orbit-coupling (SOC) via a spin−orbit-charge transfer induced intersystem crossing (SOCT-ISC) mechanism.[1]

PDI derivatized with metal complexes has also been developed.[7−14] These compounds offer many advantages such as increased solubility, highly efficient ISC owing to the presence of heavy metal ions, and long-lived triplet excited states. As Ru(II) polypyridyl complexes are also known for their excellent (photo)chemical stability and ability to sensitize the generation of singlet oxygen, they have also been very popular in the development of PDI-derivatized complexes.[14−16]

We recently addressed this issue by the facile synthesis of the $[Ru(phen)_2(pPDIp)](PF_6)_2$ dyad (RupPDIp, pPDIp = 1,10-phenanthroline chelate ligand (phen) linked to the pendant perylene diimide group).[17] RupPDIp improved the solubility of pPDIp and caused weak electronic coupling between the two moieties, maintaining the individual electronic properties and resulting in interesting photophysical properties. Upon light excitation, a charge-separated intermediate state

Scheme 1. Molecular Structures of PDI-Py Ligand, $[Ru(phen)_3]^{2+}$ Reference Complex and RuPDI-Py Dyad

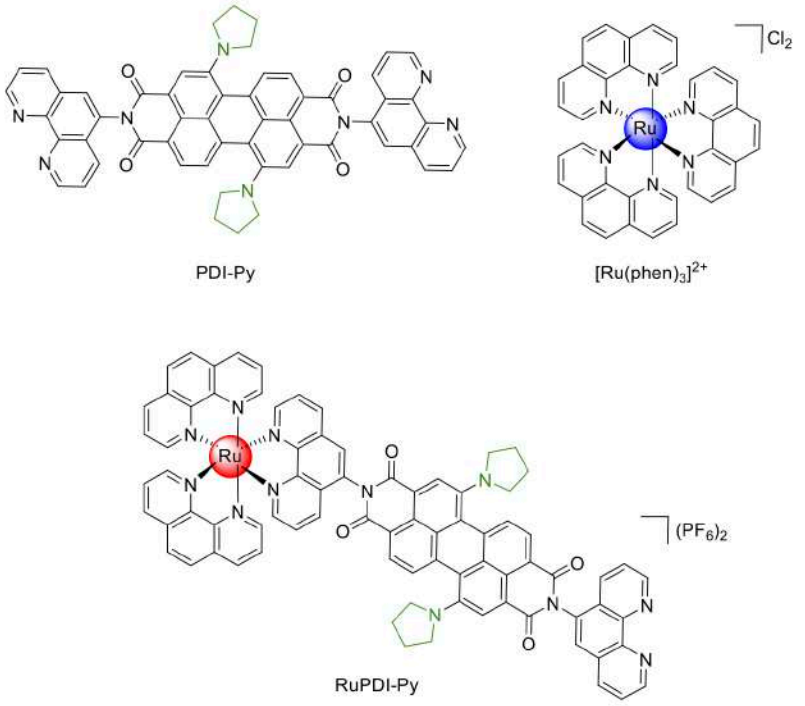

$\{(phen)_2Ru(III)(pPDIp^{\bullet-})\}$ was populated independently of the electronically excited moiety, which triggered the population of triplet state ^{3}pPDIp (τ = 1.8 μs) and photosensitized $^1O_2$ with a high quantum yield (ϕ_Δ = 0.58) in an acetonitrile solution. In an aqueous solution, the dyad exhibited the formation of H-type aggregates, and the phosphorescent emission of the $\{[Ru(phen)_3]^{2+}\}$ moiety was preserved, while the fluorescence of the pPDIp moiety was quenched. Despite the formation of aggregates, the dyad in water was still able to generate $^1O_2$ after excitation of both moieties.[18] The dyad demonstrated potential application as a photosensitizer in photodynamic therapy for melanoma cancer treatment.[18] The *in vitro* experiments showed that in the dark the dyad was not cytotoxic to B16F10-Nex2 murine melanoma cells. However, under green light illumination at 518 nm (dose = 0.41 J cm^{-2}), it exhibited a strong photocytotoxicity effect, with an IC_{50} value of 1.2 μmol L^{-1}. Despite these promising results, photochemical applications are limited by the relatively short wavelength range of 350−600 nm covered by this dyad. In this regard, the addition of electron-donating or accepting substituents in the bay position of the PDI has been used as an alternative to modifying the optical and electrochemical properties of these chromophores.[19]

Lukas et al. reported that substitution at the 1,7-bay position of PDI compounds with electron-donating groups, such as pyrrolidine (Py), resulted in a shift in the absorption and emission to the NIR region. For example, the 1,7-bis-(pyrrolidin-1-yl)-3,4:9,10-perylene-bis(dicarboximide) exhibited an intense absorption at 686 nm (ε = 46,000 M^{-1} cm^{-1}) in toluene and a fluorescence at 721 nm (Φ_{fl} = 0.65, τ_{fl} = 4.5 ns) attributed to the singlet excited state (S_1) with charge transfer (CT) character.[20]

The distinct photophysical properties of the 1,7-pyrrolidinyl-substituted perylene derivatives are associated with the electron-donating ability of the pyrrolidine substituents, which introduce a different character for the HOMO relative to the unsubstituted PDI, since the HOMO is localized on the amino nitrogen of the pyrrolidine and leads to the CT character of the PDI states.[21] Although these PDI-pyrrolidine derivatives show excellent light-harvesting properties in the NIR region, they are not able to populate the long-lived perylene diimide triplet excited state (^{3}*PDI). Therefore, different strategies have been used to reach the ^{3}*PDI state. For example, Shibano and co-workers demonstrated that a pyrrolidine-substituted PDI-C_{60} linked dyad in toluene exhibited singlet−singlet energy transfer from PDI to C_{60}, followed by intersystem crossing to the C_{60} excited triplet state and subsequent triplet−triplet energy transfer to yield the ^{3}*PDI state.[22] Another strategy involves the incorporation of transition metals into the structure of the PDI-pyrrolidine derivatives. Amati and co-workers prepared a side-to-face array DPy-gPBI[Ru(4-tBuTPP)(CO)]$_2$, based on a pyrrolidine-substituted PDI sandwiched between two Ru(II)-porphyrins, that through a photoinduced electron transfer process leads to the formation of a charge transfer state PBI^--RuP^+ (perylene anion and porphyrin radical cation) that decays to the ^{3}*PDI state (τ = 13 μs) in CH_2Cl_2.[15]

The present study extends the previous study on the $[Ru(phen)_2(pPDIp)](PF_6)_2$ dyad to a new Ru(II)-perylene dyad in which the pPDIp component is replaced by new 1,7-pyrrolidinyl-substituted perylene (PDI-Py), which consists of a perylene diimide derivatized at the 1,7-bay-positions with pyrrolidine and at the imide positions with 1,10-phenanthroline (Scheme 1). The photochemical and photophysical properties of the RuPDI-Py dyad were investigated using steady-state and time-resolved spectroscopic techniques and compared with those of the individual components, such as the PDI-Py ligand and the $[Ru(phen)_3]^{2+}$ complex, as a reference. Our results demonstrate that the coordination of PDI-Py to the $\{[Ru(phen)_3]^{2+}\}$ moiety shifts the spectroscopic features of the dyad to the visible-NIR region, providing the long-lived triplet excited state of the PDI-Py component (^{3}*PDI-Py) that

enables $^1O_2$ activation while maintaining ^{1}*PDI-Py fluorescence.

EXPERIMENTAL SECTION

General Methods and Materials. All solvents used in synthetic work and spectroscopic analysis were purchased from Sigma-Aldrich and were of HPLC grade (with the exception of Uvasol grade dimethyl sulfoxide (DMSO) from Merck used for femtosecond transient absorption analysis). The reagents were used as received without further purification. The synthetic routes and characterization of synthesized compounds are described in the Supporting Information.

Photophysical Studies. UV−vis absorption spectra were recorded with a PerkinElmer λ40 spectrophotometer using quartz cells with an optical path length of 1.0 or 5.0 cm. The emission and excitation spectra were recorded using an Edinburgh FLS920 spectrometer equipped with a Hamamatsu R928 phototube. Emission lifetimes were measured with an Edinburgh FLS920 spectrofluorometer using the time-correlated single-photon counting (TCSPC) technique. The emission quantum yield of the ligand was measured using $[Os(bpy)_3](PF_6)_2$ in deaerated acetonitrile (Φ_{EM} = 0.005) as a standard. Deaerated solutions were obtained by repeated pump−freeze−thaw cycles (~4 × 10^{-6} mbar) using sealed quartz cuvettes. Luminescence measurements at 77 K were performed in butyronitrile glass using quartz tubes.

Electrochemical Analysis. Cyclic voltammetry experiments were carried out at room temperature in argon-purged dried CH_3CN using an EcoChemie Autolab 30 potentiostat in a 3-electrode setup. The working electrode consisted of a glassy carbon electrode (3 mm diameter), the counter electrode was a Pt spiral electrodeand an Ag wire was used as quasi-reference electrode (AgQRE). Working electrode and quasi-reference electrodes were polished on a felt pad with 0.05 or 0.3 μm alumina suspension and sonicated in deionized water for 1 min before each experiment; the Pt wire was flame cleaned. Tetrabutylammonium hexafluorophosphate ($TBAPF_6$, 0.1 M) is added to the solution as a supporting electrolyte. Ferrocene (purified by sublimation at reduced pressure) is used as an internal reference ($E_{Fc+/0}$ = 0.40 V vs SCE). Spectroelectrochemical experiments were performed in an optically transparent thin-layer electrochemical (OTTLE) cell equipped with quartz windows, two Pt minigrids as working and counter electrodes, and a silver wire as a quasi-reference electrode. The solutions used for spectroelectrochemical experiments were prepared as previously described for cyclic voltammetry. UV−vis−NIR absorption spectra were recorded upon application of a given potential with an Agilent Technologies 8543 diode array spectrophotometer.

Femtosecond and Nanosecond Transient Absorption Spectroscopies. Transient absorption in the nanosecond range was performed using samples with absorbance = 0.1−0.2 at the excitation wavelength in deaerated DMSO and water solutions. A Continuum Surelite SLI-10 Nd/YAG laser was used to excite the sample with 10 ns pulses at 355 nm. The monitoring beam was supplied by an Xe arc lamp, and the signal was detected by a red-sensitive photodiode after passing through a high-radiance monochromator. Differential absorption spectra were recorded point by point, and 16 individual laser shots were averaged to improve the reliability of each acquisition. Kinetic analyses were carried out with iterative least-squares fitting procedures using OriginLab software. Global analysis has been performed with Surface Xplorer V4 software from Ultrafast Systems, by fixing principal components via single-value decomposition and by deriving the spectral distributions of the pre-exponential coefficients of the calculated lifetimes.

Transient absorption in the femtosecond range was performed by means of an Ultrafast Systems HELIOS (HE−vis−NIR) femtosecond transient absorption spectrometer using, as an excitation source, a Newport Spectra Physics Solstice-F-1K-230 V laser system, combined with a TOPAS Prime (TPR-TOPAS-F) optical parametric amplifier (pulse width: 100 fs, 1 kHz repetition rate, selected output wavelengths: 450 and 720 nm). The Solstice system was composed of a tunable (690−1040 nm) Mai Tai HP Ti/Sa femtosecond oscillator pumped by a Nd/YVO4 laser (Millennia), Ti/Sa regenerative amplifier pumped by an intracavity-doubled, Q-switched, diode-pumped Nd/YLF pulsed laser (Empower 30), optical pulse stretcher, and optical pulse compressor. The overall temporal resolution of the system is 300 fs. Air-equilibrated solutions in 0.2 cm optical path cells (absorbance at 450 and 720 nm = 0.2 nm) were analyzed under continuous stirring. To reduce the photodegradation, the pump energy of the sample was reduced to 6 μJ/pulse. Surface Xplorer V4 software from Ultrafast Systems was used for data acquisition and analysis. The 3D data surfaces were corrected for the chirp of the probe pulse prior to the analysis.

Singlet Oxygen Measurements by UV−Vis Absorption Spectroscopy. A 3 mL solution containing 100 μmol L^{-1} of the 9,10-dimethylanthracene (DMA) and 10 μmol L^{-1} of the compounds RuPDI-Py dyad, PDI-Py, and $[Ru(phen)_3]^{2+}$ complex reference in DMSO was prepared in a quartz cuvette. The initial absorbance (A_0) at 380 nm was recorded using 10 μmol L^{-1} of the respective compound in DMSO as a reference solution. The mixture was then irradiated with 450 and 720 nm lamps, and the absorbance (A_t) at 380 nm was measured at predetermined time intervals.

RESULTS AND DISCUSSION

Synthesis and Characterization. The molecular structures of the PDI-Py ligand, the RuPDI-Py dyad, and $[Ru(phen)_3]^{2+}$ are shown in Scheme 1. The synthesis of the PDI-Py ligand was adapted from the previously reported methods for the structurally bay-substituted PDI compounds.[23,24] The RuPDI-Py dyad was prepared by the reaction between the PDI-Py ligand and the precursor *cis*-$[Ru(phen)_2Cl_2]$ in DMF, as described in the Supporting Information. Structural characterization of PDI-Py and RuPDI-Py was obtained by ESI-MS (mass spectrometry) (Figures S1 and S6) and one- and two-dimensional NMR spectroscopy (Figures S2−S5 and S7−S10).

The ESI-MS spectrum confirms the structures and purity of the synthesized compounds. The molecular ion peaks appeared at m/z 885.2954 $[M + H]^+$ and 443.1521 $[M + 2H]^{2+}$ for the PDI-Py ligand and at m/z 673.1649 $[M]^{2+}$ and 443.1521 $[M + H]^{3+}$ for the RuPDI-Py. The combined 1D and 2D-NMR experiments allowed ^{1}H and ^{13}C signal attribution, and the integration ratios for PDI-Py and RuPDI-Py (Tables S1 and S2) were consistent with the proposed structures.

Figure 1 shows a comparison of the aromatic regions of the ^{1}H NMR spectra of the PDI-Py ligand, the $[Ru(phen)_3]^{2+}$ reference, and the RuPDI-Py dyad. The aromatic protons of phenanthroline and the PDI core were observed in the region of 9.4−7.6 ppm. The symmetric structures of 1,7-dipyrrolidinyl substituted perylene generally show a pattern in the ^{1}H NMR spectrum characterized by three signals, a singlet and two doublets, in the range of 8.0−9.0 ppm and each signal with an area corresponding to two hydrogens, indicating that there are only three types of different kinds of protons in the perylene core.[25] This signal pattern was observed for the PDI-Py ligand (H_a, H_b, and H_c), demonstrating that the symmetry of the molecule was preserved after the addition of phenanthroline substituents and that the pyrrolidines were localized in the 1,7-bay positions. As observed in the spectrum of the RuPDI-Py dyad, the pattern of signals is characteristic of $[Ru(phen)_3]^{2+}$ and free PDI-Py moieties and the PDI-Py moiety to Ru metal. The chemical shifts of the signals from the phen ligands of the RuPDI-Py dyad are similar to those of the signals from the phen ligands of the $[Ru(phen)_3]^{2+}$ complex. Likewise, as observed the moiety of free moieties of the PDI-Py ligand,

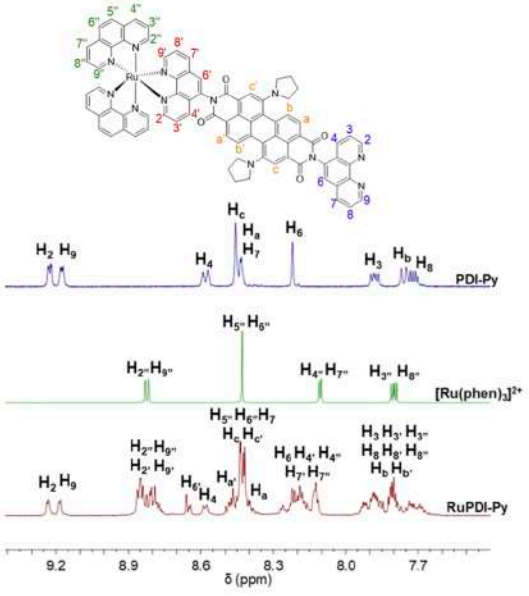

Figure 1. Aromatic region of the ^{1}H NMR spectra with proton assignment for compounds PDI-Py, $[Ru(phen)_3]^{2+}$, and RuPDI-Py in DMSO-d_6.

whereas the moiety of the PDI-Py ligand bound to Ru also shows signals similar to phen ligands.

Spectroscopic Studies in DMSO. The absorption and emission spectra of the RuPDI-Py dyad and corresponding reference compounds in DMSO are shown in Figure 2 and the data are summarized in Table 1. The absorption of the PDI-Py ligand is characterized by two absorption bands at 420 and 720 nm (Figure 2A), attributed to the $S_0 \rightarrow S_2$ and $S_0 \rightarrow S_1$ electronic transitions, respectively. These data are consistent with previous literature data on similar compounds.[21,25−27] The substitution at the bay positions resulted in a bathochromic shift of the absorption maxima (~185 nm), and the loss of three characteristic vibronic absorption bands observed in core-unsubstituted pPDIp ligand.[17]

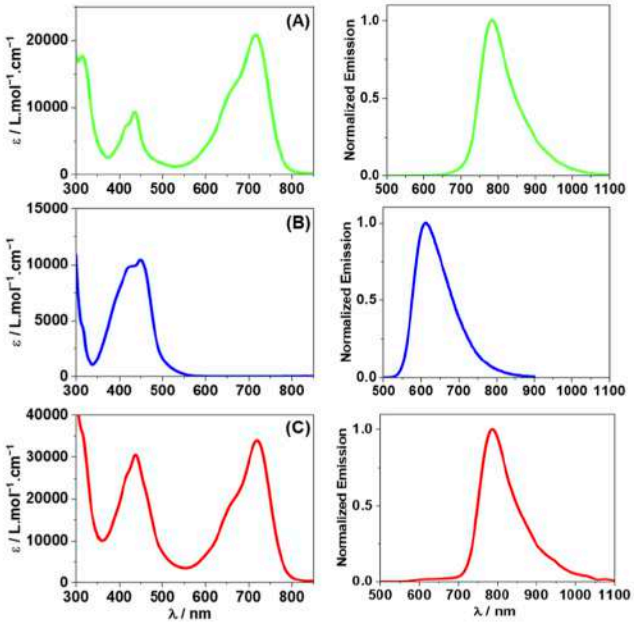

Figure 2. Absorption and emission (λ_{EX} = 420 nm) spectra of the PDI-Py ligand (A), $[Ru(phen)_3]^{2+}$ (B), and RuPDI-Py dyad (C) in deaerated DMSO solution (c = 20 μmol L^{-1}).

Table 1. Photophysical Properties in DMSO Solution

compound	λ_{Abs}, nm (ε, M^{-1} cm^{-1})	λ_{EM}, nm	τ_{EM}, ns	Φ_{EM}
PDI-Py	435 (9300)	767	1.75	0.03
	720 (20,700)			
RuPDI-Py	435 (30,100)	776	1.50	
	720 (33,900)			
$[Ru(phen)_3]^{2+}$	450 (10,450)	610	1025[a]	0.11[a]

[a]Deaerated solutions.

The PDI-Py reference displayed an emission band with a maximum at 780 nm, which originates from the lowest singlet excited state (S_1). The emission spectrum was independent of the presence of oxygen, and the excitation spectrum corresponded to the absorption spectrum (Figure S11). The fluorescence lifetime and fluorescence quantum yield were lower than those observed for pPDIp (τ_{fl} = 3.5 ns and Φ_{fl} = 0.97 in DMF).[17] According to the literature,[20,22,26] pyrrolidine bay-substituted perylene compounds exhibit low fluorescence quantum yields and short fluorescence lifetimes in polar solvents, due to the intramolecular charge transfer (CT) character of the lowest excited state.

The absorption spectrum of the RuPDI-Py dyad preserves the low-energy absorption of the PDI-Py chromophore at 720 nm, whereas the absorption band at 440 nm can be attributed to the contributions of both PDI-Py and $[Ru(phen)_3]^{2+}$ chromophores. The emission spectrum of the RuPDI-Py dyad is independent of the photoexcitation wavelength (350−700 nm) and of the presence of oxygen and resembles that of the PDI-Py chromophore. However, it presents a small red-shift of the maximum absorption (~9 nm), and the fluorescence lifetime of τ_{em} = 1.50 ns is shorter than that observed for the PDI-Py reference (Table 1 and Figure S12).

To confirm the solvatochromic behavior of the $S_0 \rightarrow S_1$ electronic transition, the absorption and emission features of PDI-Py and RuPDI-Py were measured in various solvents of different polarities at room temperature and in a glass matrix at 77 K (Figure S14). The absorption spectra of both compounds were not significantly influenced by the solvent, whereas the fluorescence spectra were blue-shifted in the nonpolar solvents. For more details, see S4 in the Supporting Information.

Notably, the intense and long-lived emission arising from the ^{3}MLCT state of the $\{[Ru(phen)_3]^{2+}\}$ chromophore was completely quenched in the dyad in all organic solvents evaluated. These results differ from those previously observed for the $[Ru(phen)_2(pPDIp)]$ dyad,[17] which exhibited the emission of both $\{[Ru(phen)_3]^{2+}\}$ and {pPDIp} chromophores.

Quenching of ^{3}MLCT of the $\{[Ru(phen)_3]^{2+}\}$ moiety may be related to electron transfer from the $\{[Ru(phen)_3]^{2+}\}$ to the {PDI-Py} unit.[22,28] The energy transfer process was ruled out by comparison of the excitation and absorption spectra (Figure S11) and by comparison of the PDY-Py fluorescence of optically matched solutions of the RuPDI-Py dyad and PDI-Py (Figure S13). To gain further insights into the quenching process, femtosecond (pump−probe) and nanosecond (flash-photolysis) transient absorption methods were used to investigate the excited-state properties of the PDI-Py ligand, the RuPDI-Py dyad, and $[Ru(phen)_3]^{2+}$ in DMSO solution. The samples were excited at 720 nm, where only PDI-Py

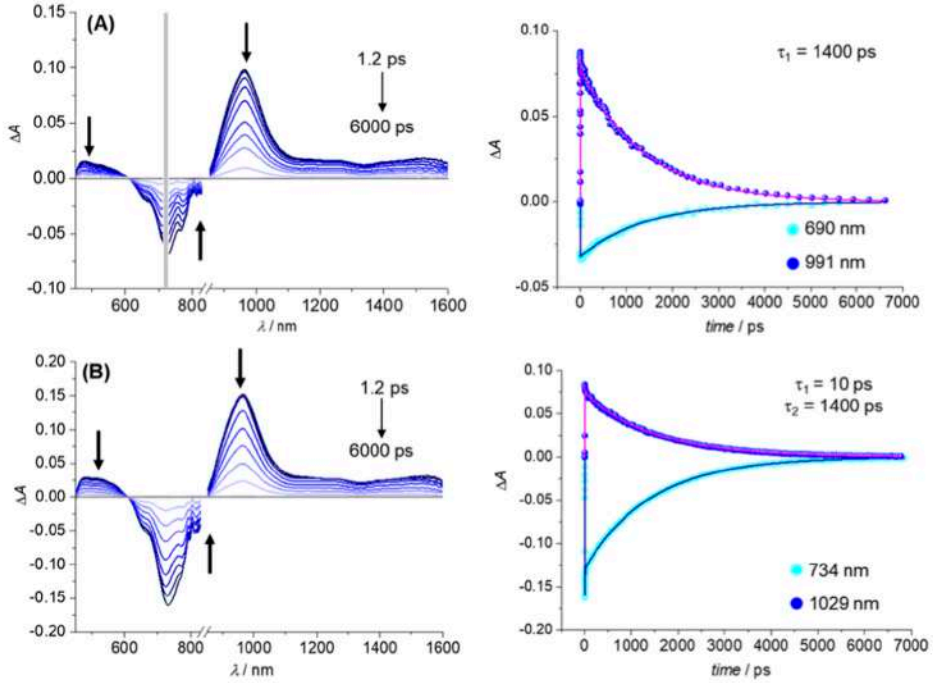

Figure 3. Femtosecond transient absorption spectroscopy of the PDI-Py ligand with λ_{exc} = 720 nm (A) and 450 nm (B) in DMSO: spectral evolution and kinetic analysis at selected wavelengths.

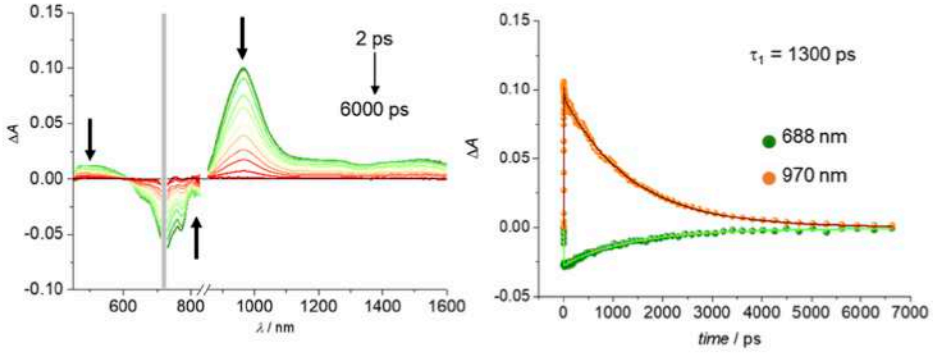

Figure 4. Femtosecond transient absorption spectroscopy of the RuPDI-Py dyad with λ_{exc} = 720 nm in DMSO: spectral evolution and kinetic analysis at selected wavelengths.

absorbs, and at 355 or 450 nm, where both the {PDI-Py} and {[Ru(phen)$_3$]$^{2+}$} moieties absorb light.

The transient absorption spectra of the PDI-Py ligand (Figure 3), obtained with λ_{exc} of 450 and 720 nm, are characterized by excited-state absorption with maxima at 480 and 963 nm and broad features up to 1600 nm and by negative bands with peaks at 720 and 770 nm, assigned to ground-state bleaching and stimulated emission, respectively. The isosbestic points at 680 and ca. 840 nm indicate the presence of one process and the absorption decay is characterized by a lifetime of 1.40 ns all over the spectral range, in reasonable agreement with the lifetime of 1.75 ns measured from luminescence experiments. The observed features can thus be ascribed to the lowest singlet excited state of PDI-Py. Upon excitation at 450 nm, a short lifetime of 10 ps preceding the decay of 1.40 ns is observed (Figure 3B), which is attributable to $S_2 \rightarrow S_1$ internal conversion. The observed transient absorption spectrum of PDI-Py is similar to that reported for the singlet excited state of pyrrolidine-substituted perylene compounds.[15,22,29−31] The features of the triplet excited state of PDI-Py were not visible in both picosecond and nanosecond time-regime measurements.

The transient spectrum of the RuPDI-Py dyad recorded after selective excitation of the PDI-Py component at 720 nm (Figure 4) shows spectral features identical to those exhibited by the PDI-Py ligand, indicating the formation of the singlet excited state ^{1}PDI-Py. The kinetic analysis demonstrates a slightly shorter lifetime (1.30 ns) compared to that of the PDI-Py model, as already reported in Table 1 for luminescence intensity decays (τ_{fl} = 1.50 ns).

The transient spectral changes obtained following the 450 nm excitation of the RuPDI-Py dyad differ from those observed upon excitation of the PDI-Py model. Three families of curves, characterized by different isosbestic points, are identified (Figure 5). The end-of-pulse spectrum in Figure 5A shows features of both components: a positive broad absorption at 534 nm is attributed to the ^{3}MLCT state of the {[Ru(phen)$_3$]$^{2+}$} moiety (by comparison with the spectrum exhibited by the [Ru(phen)$_3$]$^{2+}$ reference, Figure S15a) while the bleaching at 730 nm and the positive

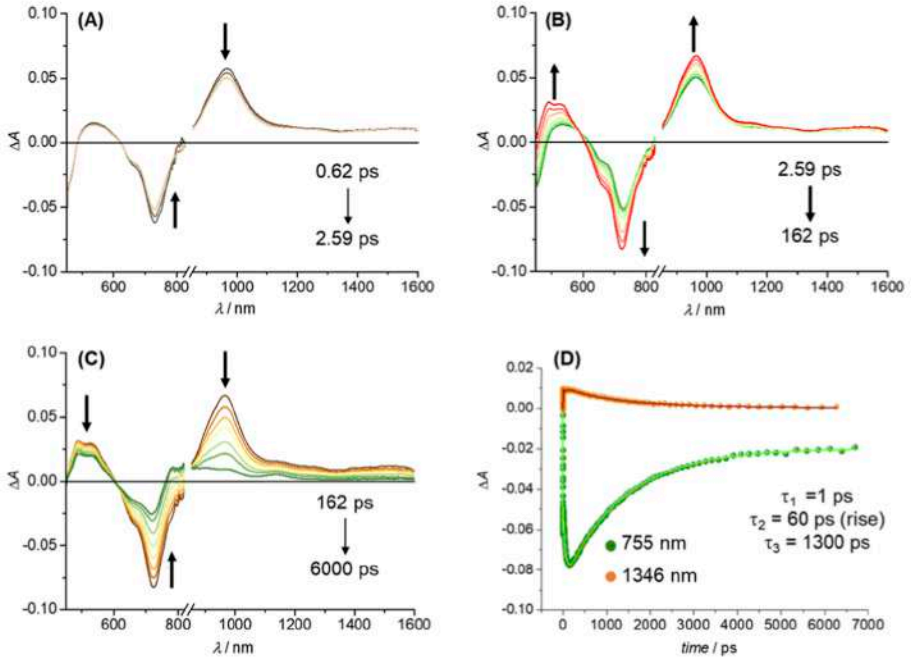

Figure 5. Femtosecond transient absorption spectroscopy of the RuPDI-Py dyad with λ_{exc} = 450 nm in DMSO: spectral evolution and kinetic analysis at selected wavelengths.

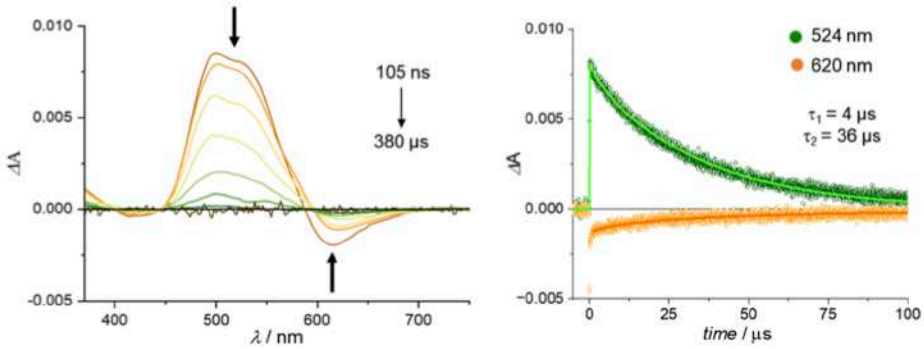

Figure 6. Nanosecond transient absorption spectroscopy of the RuPDI-Py dyad (λ_{exc} = 355 nm) in DMSO under oxygen-free conditions: spectral evolution and kinetic traces at 524 and 620 nm.

absorption at 963 nm are characteristic of the PDI-py chromophore (the negative band appears less structured due to the absence of stimulated emission at 770 nm). This first fast process (lifetime on the order of 1 ps) leads to small spectral variations and is probably due to solvent-induced relaxation. During the next step (2.59−162 ps, Figure 5B), the spectral evolution is characterized by the rise of a species with a structured absorption in the 450−600 nm region, ground-state bleaching, and positive absorption in the NIR region. The time constant of this process is 60 ps, and the isosbestic point at 580 nm indicates the interdependence of the two species involved in the absorption. On a longer time scale (up to 6000 ps) in Figure 5C, the spectrum decays with the same kinetics observed for 720 nm excitation (τ = 1.30 ns), indicating the decay of the ^{1}PDI-Py state, due to the direct excitation of the chromophore in the dyad (approximately 50%). It is interesting to note that the last spectrum exhibits a small positive band at 800 nm and peaks at 490 and 530 nm, suggesting that the new species formed in 60 ps remains on longer time scales. This species can be attributed to the charge-separated (CS) state {Ru^{3+}-(PDI-$Py^{\bullet-}$)}, by considering that the radical anion of perylene diimide units substituted with pyrrolidine is characterized by an absorption peak at 800 nm,[15,32] and by comparison with the spectral features obtained from UV−vis spectroelectrochemistry upon reduction of the RuPDI-Py dyad (Figure S18).

Nanosecond transient absorption spectroscopy was performed to obtain precise information about the long-lived states in the dyad (Figure 6). The initial spectrum displays a structured positive absorption between 450 and 600 nm and ground-state bleaching between 600 and 700 nm. It can be noticed that the structure of the band in the 450−600 region disappears over time, leaving a broadband peaked at 500 nm. Furthermore, different isosbestic points are present in the 450−600 nm region: 575 nm in the time interval 105 ns to 2 μs and 595 nm above 10 μs. This demonstrates that two consecutive processes are in place. A global fit analysis (Figure S16) with two components yielded two lifetimes of 4 and 36 μs: the spectral distribution of the lifetimes' amplitudes reveals that the species that lives 4 μs shows the features of the {Ru^{3+}-(PDI-$Py^{\bullet-}$)} CS state, while the species with τ = 36 μs can be attributed to the triplet state ^{3}PDI-Py. The latter spectral

features, in fact, are compatible with those reported for the triplet excited state of PDI bay-substituted compounds.[15,22,30] Population of the PDI-Py triplet state from deactivation of the CS state can be speculated but cannot be experimentally determined due to the extensive overlay of the signals.

A qualitative energy–level diagram describing the photophysics of the RuPDI-Py dyad is presented in Scheme 2. The

Scheme 2. Qualitative Energy–Level Diagram of RuPDI-Py Dyad in DMSO[a]

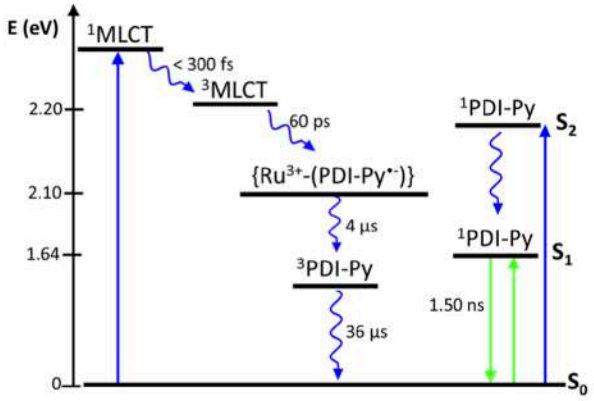

[a]Blue: excitation at 450 nm; green: excitation at 720 nm. Estimation of the CS level on the basis of electrochemical data (Table S3).

excitation of {PDI-Py} at 720 nm results in the population of the ^{1}PDI-Py state, which decays with fluorescence at 780 nm. The population of ^{1}MLCT is followed by efficient ISC to ^{3}MLCT. The quenching of the ^{3}MLCT luminescence can be attributed to electron transfer from the $\{Ru(phen)_3\}^{2+}$ moiety to the {PDI-Py} component, through the formation of the CS intermediate state $\{Ru^{3+}\text{-PDI-Py}^{\bullet-}\}$ in 60 ps. The CS state decays with a lifetime of 4 μs to generate a long-lived triplet state ^{3}PDI-Py (36 μs). It is important to emphasize that the formation of the long-lived ^{3}PDI-Py state was observed only in the RuPDI-Py dyad upon excitation of the $\{Ru(phen)_3\}^{2+}$ moiety, and there was no evidence of its generation in the PDI-Py ligand, reinforcing the importance of the participation of the Ru(II) metal center in the process.

Singlet Oxygen Photogeneration. The singlet oxygen ($^1O_2$) photogeneration capacity of the RuPDI-Py dyad, the PDI-Py ligand, and $[Ru(phen)_3]^{2+}$ in DMSO was evaluated using 9,10-dimethylanthracene (DMA) as a quencher of $^1O_2$. According to the literature,[33] DMA absorption would be bleached upon the chemical quenching reaction of DMA with $^1O_2$. Figures 7, S18 and S19 show the UV–vis spectral evolution of a DMA solution in DMSO recorded during the irradiation of the compounds using 450 and 720 nm light.

Irradiation of the RuPDI-Py dyad at 450 nm decreases the absorption of DMA at 380 nm, indicating its reaction with $^1O_2$ photogenerated by this compound. In contrast, irradiation at 720 nm does not result in DMA spectral changes, demonstrating that this excitation wavelength cannot photosensitize $^1O_2$ generation. These results indicate that the ^{3}PDI-Py state is probably responsible for the photosensitization of $^1O_2$ via an energy-transfer process and corroborates the transient data, where the formation of the triplet state was observed only after excitation at 450 nm. Irradiation of the PDI-Py ligand at 450 and 720 nm did not cause any change in the DMA absorption spectrum, demonstrating that the free

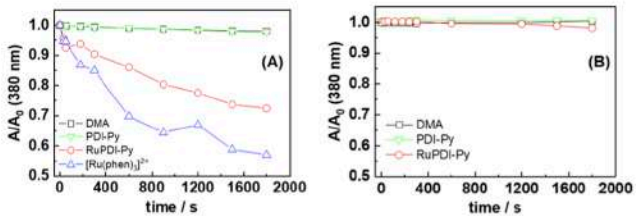

Figure 7. Bleaching of DMA in DMSO upon irradiation at 450 nm (A) and 720 nm (B) in the presence of the RuPDI-Py dyad, PDI-Py ligand, and $[Ru(phen)_3]^{2+}$. A solution containing DMA was used as a control.

ligand was not able to generate $^1O_2$ and that the formation of the triplet excited state responsible for $^1O_2$ sensitization did not occur, as observed in the transient absorption results.

CONCLUSIONS

The photophysical properties and excited-state dynamics of the RuPDI-Py dyad suggest that the electron-donating ability of pyrrolidine at the PDI bay position, phenanthroline substitutions at the PDI imide positions, and coordination to the $\{Ru(phen)_3\}$ moiety significantly influence the photophysics of both chromophores. The presence of pyrrolidine at the bay positions mainly causes an increase in the HOMO energy level, whereas the presence of 1,10-phenanthroline (acceptor group) at the imide position contributes greatly to a decrease in the LUMO energy and increases the distortion of PDI planarity. These effects decrease the HOMO–LUMO energy gap and bring closer the MLCT and PDI-Py electronic transitions, resulting in changes in the photophysical properties of the dyad. The coordination of PDI-Py to the $\{Ru(phen)_3\}^{2+}$ moiety is crucial for establishing an electron transfer process between the $\{(Ru(phen)_3)^{2+}\}$ and the {PDI-Py} components generating a CS state which subsequently populates the ^{3}PDI-Py state that decays with a long lifetime. Herein we obtained a NIR luminescent material that shows unique photophysical properties dependent on the excitation wavelength. The dyad presents multifunctional properties for simultaneous diagnosis in the infrared region and treatment with a significant generation of $^1O_2$, which prompts its use in photomedicine applications.

ASSOCIATED CONTENT

Supporting Information

The Supporting Information is available free of charge at https://pubs.acs.org/doi/10.1021/acs.inorgchem.3c04145.

Synthetic procedures, characterization data for all the compounds, including NMR and mass spectra, and supplementary spectroscopic data (PDF)

AUTHOR INFORMATION

Corresponding Authors

Paola Ceroni – *Dipartimento di Chimica "Giacomo Ciamician", Alma Mater Studiorum - Università di Bologna, 40126 Bologna, Italy;* orcid.org/0000-0001-8916-1473; Email: paola.ceroni@unibo.it

Rose M. Carlos – *Departamento de Química, Universidade Federal de São Carlos, São Carlos CEP 13565-905 São Paulo, Brazil;* orcid.org/0000-0002-0277-9789; Email: rosem@ufscar.br

Authors

Isabele S. Campos − *Departamento de Química, Universidade Federal de São Carlos, São Carlos CEP 13565-905 São Paulo, Brazil*

Andrea Fermi − *Dipartimento di Chimica "Giacomo Ciamician", Alma Mater Studiorum - Università di Bologna, 40126 Bologna, Italy;* orcid.org/0000-0003-1080-0530

Barbara Ventura − *Institute for Organic Synthesis and Photoreactivity (ISOF), National Research Council of Italy (CNR), I-40129 Bologna, Italy;* orcid.org/0000-0002-8207-1659

Carlos A. F. Moraes − *Departamento de Química, Universidade Federal de São Carlos, São Carlos CEP 13565-905 São Paulo, Brazil*

Gabriel H. Ribeiro − *Departamento de Química, Universidade Federal de São Carlos, São Carlos CEP 13565-905 São Paulo, Brazil;* orcid.org/0000-0003-0738-1638

Tiago Venâncio − *Departamento de Química, Universidade Federal de São Carlos, São Carlos CEP 13565-905 São Paulo, Brazil;* orcid.org/0000-0002-5592-3940

Complete contact information is available at: https://pubs.acs.org/10.1021/acs.inorgchem.3c04145

Author Contributions

The manuscript was written through contributions of all authors. All authors have given approval to the final version of the manuscript.

Notes

The authors declare no competing financial interest.

ACKNOWLEDGMENTS

This work was funded by the São Paulo Research Foundation (FAPESP), grants #2018/03424-0, #2021/10586-9, and #2022/066370, CNPq 307464/2021-0, CAPES (under finance code 001).

REFERENCES

(1) Deckers, J.; Cardeynaels, T.; Lutsen, L.; Champagne, B.; Maes, W. Heavy-Atom-Free Bay-Substituted Perylene Diimide Donor-Acceptor Photosensitizers. *ChemPhysChem* **2021**, *22* (14), 1488−1496.

(2) Fang, S.; Zhou, J.; Zhou, X.; Wang, C.; Jiang, N.; Liu, L.; Xie, Z. Interchromophore Rotation-Related Ultrafast Charge Separation at Excited States in Head-to-Tail Linked Perylene Diimide Dyads. *J. Phys. Chem. C* **2019**, *123* (38), 23306−23311.

(3) Liu, X.; Hu, M.; Li, Y.; Zhao, X.; Zhang, Y.; Hu, Y.; Yuan, Z.; Chen, Y. 1,2,4-Triazoline-3,5-Dione Substituted Perylene Diimides as near Infrared Acceptors for Bulk Heterojunction Organic Solar Cells. *Dyes Pigm.* **2021**, *187*, 109108.

(4) Lee, K. J.; Woo, J. H.; Kim, E.; Xiao, Y.; Su, X.; Mazur, L. M.; Attias, A.-J.; Fages, F.; Cregut, O.; Barsella, A.; Mathevet, F.; Mager, L.; Wu, J. W.; D'Aléo, A.; Ribierre, J.-C. Electronic Energy and Electron Transfer Processes in Photoexcited Donor-Acceptor Dyad and Triad Molecular Systems Based on Triphenylene and Perylene Diimide Units. *Phys. Chem. Chem. Phys.* **2016**, *18* (11), 7875−7887.

(5) Barendt, T. A.; Myers, W. K.; Cornes, S. P.; Lebedeva, M. A.; Porfyrakis, K.; Marques, I.; Félix, V.; Beer, P. D. The Green Box: An Electronically Versatile Perylene Diimide Macrocyclic Host for Fullerenes. *J. Am. Chem. Soc.* **2020**, *142* (1), 349−364.

(6) Schulze, M.; Steffen, A.; Würthner, F. Near-IR Phosphorescent Ruthenium(II) and Iridium(III) Perylene Bisimide Metal Complexes. *Angew. Chem., Int. Ed.* **2015**, *54* (5), 1570−1573.

(7) Işık Büyükekşi, S.; Karatay, A.; Acar, N.; Küçüköz, B.; Elmali, A.; Şengül, A. Electron/Energy Transfer Studies on Hybrid Materials Based on Dinuclear Coordination Compounds of Twisted Perylene Diimide. *J. Photochem. Photobiol., A* **2019**, *372*, 226−234.

(8) Mauri, L.; Colombo, A.; Dragonetti, C.; Fagnani, F.; Roberto, D. Iridium and Ruthenium Complexes Bearing Perylene Ligands. *Molecules* **2022**, *27*, 7928.

(9) Schulze, M.; Steffen, A.; Würthner, F. Near-IR Phosphorescent Ruthenium(II) and Iridium(III) Perylene Bisimide Metal Complexes. *Angew. Chem., Int. Ed.* **2015**, *54* (5), 1570−1573.

(10) Danilov, E. O.; Rachford, A. A.; Goeb, S.; Castellano, F. N. Evolution of the Triplet Excited State in Pt^{II} Perylenediimides. *J. Phys. Chem. A* **2009**, *113* (19), 5763−5768.

(11) Mauri, L.; Colombo, A.; Dragonetti, C.; Fagnani, F.; Roberto, D. Iridium and Ruthenium Complexes Bearing Perylene Ligands. *Molecules* **2022**, *27*, 7928.

(12) Yip, A. M. H.; Shum, J.; Liu, H. W.; Zhou, H.; Jia, M.; Niu, N.; Li, Y.; Yu, C.; Lo, K. K. W. Luminescent Rhenium(I)-Polypyridine Complexes Appended with a Perylene Diimide or Benzoperylene Monoimide Moiety: Photophysics, Intracellular Sensing, and Photocytotoxic Activity. *Chem.—Eur. J.* **2019**, *25* (38), 8970−8974.

(13) Weissman, H.; Shirman, E.; Ben-Moshe, T.; Cohen, R.; Leitus, G.; Shimon, L. J. W.; Rybtchinski, B. Palladium Complexes of Perylene Diimides: Strong Fluorescence despite Direct Attachment of Late Transition Metals to Organic Dyes. *Inorg. Chem.* **2007**, *46* (12), 4790−4792.

(14) Dubey, R. K.; Niemi, M.; Kaunisto, K.; Stranius, K.; Efimov, A.; Tkachenko, N. V.; Lemmetyinen, H. Excited-State Interaction of Red and Green Perylene Diimides with Luminescent Ru(II) Polypyridine Complex. *Inorg. Chem.* **2013**, *52* (17), 9761−9773.

(15) Amati, A.; Natali, M.; Indelli, M. T.; Iengo, E.; Würthner, F. Photoinduced Energy- and Electron-Transfer Processes in a Side-to-Face RuII-Porphyrin/Perylene-Bisimide Array. *ChemPhysChem* **2019**, *20* (17), 2195−2203.

(16) Mari, C.; Huang, H.; Rubbiani, R.; Schulze, M.; Würthner, F.; Chao, H.; Gasser, G. Evaluation of Perylene Bisimide-Based Ru^{II} and Ir^{III} Complexes as Photosensitizers for Photodynamic Therapy. *Eur. J. Inorg. Chem.* **2017**, *2017* (12), 1745−1752.

(17) Santos, E. R. D.; Pina, J.; Venâncio, T.; Serpa, C.; Martinho, J. M. G.; Carlos, R. M. Photoinduced Energy and Electron-Transfer Reactions by Polypyridine Ruthenium(II) Complexes Containing a Derivatized Perylene Diimide. *J. Phys. Chem. C* **2016**, *120* (40), 22831−22843.

(18) de Campos, I. A. S.; dos Santos, E. R.; Sellani, T. A.; Herbozo, C. C. A.; Rodrigues, E. G.; Roveda, A. C.; Pazin, W. M.; Ito, A. S.; Santana, V. T.; Nascimento, O. R.; Carlos, R. M. Influence of the Medium on the Photochemical and Photophysical Properties of [Ru(Phen)2(PPDIp)]2+. *ChemPhotoChem* **2018**, *2* (8), 757−764.

(19) Huang, C.; Barlow, S.; Marder, S. R. Perylene-3,4,9,10-Tetracarboxylic Acid Diimides: Synthesis, Physical Properties, and Use in Organic Electronics. *J. Org. Chem.* **2011**, *76* (8), 2386−2407.

(20) Lukas, A. S.; Zhao, Y.; Miller, S. E.; Wasielewski, M. R. Biomimetic Electron Transfer Using Low Energy Excited States: A Green Perylene-Based Analogue of Chlorophyll a. *J. Phys. Chem. B* **2002**, *106* (6), 1299−1306.

(21) Würthner, F.; Saha-Möller, C. R.; Fimmel, B.; Ogi, S.; Leowanawat, P.; Schmidt, D. Perylene Bisimide Dye Assemblies as Archetype Functional Supramolecular Materials. *Chem. Rev.* **2016**, *116* (3), 962−1052.

(22) Shibano, Y.; Umeyama, T.; Matano, Y.; Tkachenko, N. V.; Lemmetyinen, H.; Araki, Y.; Ito, O.; Imahori, H. Large Reorganization Energy of Pyrrolidine-Substituted Perylenediimide in Electron Transfer. *J. Phys. Chem. C* **2007**, *111* (16), 6133−6142.

(23) Würthner, F.; Stepanenko, V.; Chen, Z.; Saha-Möller, C. R.; Kocher, N.; Stalke, D. Preparation and Characterization of Regioisomerically Pure 1,7-Disubstituted Perylene Bisimide Dyes. *J. Org. Chem.* **2004**, *69* (23), 7933−7939.

(24) Işık Büyükekşi, S.; Şengül, A.; Erdönmez, S.; Altındal, A.; Orman, E. B.; Özkaya, A. R. Spectroscopic, Electrochemical and Photovoltaic Properties of Pt(II) and Pd(II) Complexes of a

Chelating 1,10-Phenanthroline Appended Perylene Diimide. *Dalton Trans.* **2018**, *47* (8), 2549−2560.
(25) Dubey, R. K.; Efimov, A.; Lemmetyinen, H. 1,7-And 1,6-Regioisomers of Diphenoxy and Dipyrrolidinyl Substituted Perylene Diimides: Synthesis, Separation, Characterization, and Comparison of Electrochemical and Optical Properties. *Chem. Mater.* **2011**, *23* (3), 778−788.
(26) Ozser, M. E.; Sarkodie, S. A.; Mohiuddin, O.; Ozesme, G. Novel Derivatives of Regioisomerically Pure 1,7-Disubstituted Perylene Diimide Dyes Bearing Phenoxy and Pyrrolidinyl Substituents: Synthesis, Photophysical, Thermal, and Structural Properties. *J. Lumin.* **2017**, *192*, 414−423.
(27) Leowanawat, P.; Nowak-Król, A.; Würthner, F. Tetramethoxy-Bay-Substituted Perylene Bisimides by Copper-Mediated Cross-Coupling. *Org. Chem. Front.* **2016**, *3* (5), 537−544.
(28) Dubey, R. K.; Inan, D.; Sengupta, S.; Sudhölter, E. J. R.; Grozema, F. C.; Jager, W. F. Tunable and Highly Efficient Light-Harvesting Antenna Systems Based on 1,7-Perylene-3,4,9,10-Tetracarboxylic Acid Derivatives. *Chem. Sci.* **2016**, *7* (6), 3517−3532.
(29) Dubey, R. K.; Niemi, M.; Kaunisto, K.; Efimov, A.; Tkachenko, N. V.; Lemmetyinen, H. Direct Evidence of Significantly Different Chemical Behavior and Excited-State Dynamics of 1,7- and 1,6-Regioisomers of Pyrrolidinyl-Substituted Perylene Diimide. *Chem.—Eur. J.* **2013**, *19* (21), 6791−6806.
(30) Supur, M.; El-Khouly, M. E.; Seok, J. H.; Kim, J. H.; Kay, K. Y.; Fukuzumi, S. Efficient Electron Transfer Processes of the Covalently Linked Perylenediimide-Ferrocene Systems: Femtosecond and Nanosecond Transient Absorption Studies. *J. Phys. Chem. C* **2010**, *114* (24), 10969−10977.
(31) Indelli, M. T.; Chiorboli, C.; Scandola, F.; Iengo, E.; Osswald, P.; Würthner, F. Photoinduced Processes in Self-Assembled Porphyrin/Perylene Bisimide Metallosupramolecular Boxes. *J. Phys. Chem. B* **2010**, *114* (45), 14495−14504.
(32) Goretzki, G.; Davies, E. S.; Argent, S. P.; Alsindi, W. Z.; Blake, A. J.; Warren, J. E.; McMaster, J.; Champness, N. R. Bis-Morpholine-Substituted Perylene Bisimides: Impact of Isomeric Arrangement on Electrochemical and Spectroelectrochemical Properties. *J. Org. Chem.* **2008**, *73* (22), 8808−8814.
(33) Hong, X.-L.; Li, H.; Peng, C.-H. Synthesis, DNA-Binding, DNA-Photocleavage and Antioxidant Activity of Ruthenium(II) Complex Containing Triazine Ring Ligand: [Ru(Dmb)2(Pdta)]-(ClO4)2. *J. Mol. Struct.* **2011**, *990* (1−3), 197−203.